Cellular Physiology and Biochemistry

Cell Physiol Biochem 2018;49:1659-1676
DOI: 10.1159/000493502
Published online: 14 September, 2018
Accepted: 5 September, 2018

Original Paper

miR-26a/HOXC9 Dysregulation Promotes Metastasis and Stem Cell-Like Phenotype of Gastric Cancer

Xudong Peng Qingjie Kang Rui Wan Ziwei Wang

Gastrointestinal Surgical Unit, the First Affiliated Hospital of Chongqing Medical University, Chongqing, China

Key Words
Hoxc9 • Gastric cancer • Metastasis • Stem cell-like phenotype

Abstract
Background/Aims: Previous studies demonstrated that HOXC9 acts as an oncogene in several tumors. The aim of this study was to explore whether HOXC9 promotes gastric cancer (GC) progression and elucidate the underlying molecular mechanisms. ***Methods:*** HOXC9 expression in GC tissues and adjacent non-cancer tissues was detected by quantitative RT-PCR (qRT-PCR) and immunohistochemistry. The functional effects of HOXC9 on proliferation, metastasis and stem cell-like phenotype were evaluated by relevant experiments in GC cells. The effect of miR-26a on HOXC9 was investigated by gain- and loss-of-function assays and luciferase reporter assay. Nude mouse models were established to test the effect of miR-26a and HOXC9 on tumorigenesis and metastasis of GC cells *in vivo*. ***Results:*** Herein, we showed that HOXC9 was upregulated in GC tissues and associated with a poor prognosis. HOXC9 knockdown inhibited the metastasis and stem cell-like phenotype of GC cells without significant effects on cell proliferation. In addition, we identifed HOXC9 as a direct target of miR-26a. Restoration of miR-26a in GC cells downregulated HOXC9 and reversed its promoting effect on metastasis and self-renewal, whereas miR-26a silencing upregulated HOXC9. *In vivo* experiments showed that HOXC9 knockdown suppressed tumorigenesis and lung metastasis of GC cells in nude mice, and these effects were mimicked by restoration of miR-26a. ***Conclusion:*** The present study demonstrates that HOXC9 promotes the metastasis and stem cell-like phenotype of GC cells, and this phenomenon can be reversed by restoration of miR-26a.

Introduction

Gastric cancer (GC) is the most common gastrointestinal cancer. Approximately 900, 000 new cases and 700, 000 deaths are reported in the world every year. Despite the existence of comprehensive treatment based on surgery and chemotherapy, the 5-year survival rate of GC patients remains below 40%. Recurrence and metastasis are the main factors leading to

Ziwei Wang
Gastrointestinal Surgical Unit, the First Affiliated Hospital of Chongqing Med. Univ.
Chongqing, 400000 (China)
Tel. +86- 023-89011182, E-Mail wangziwei571@sina.com

the poor prognosis of GC patients [1]. In the past few decades, molecular targeted therapy has become an alternative therapeutic approach with the in-depth study of molecular mechanism of tumor progression. For example, a monoclonal antibody against VEGFR2 called ramucirumab and a monoclonal antibody against HER2 called trastuzumab have been used in the clinical treatment of GC [2, 3]. However, we are still far from identifying a radical cure for GC. To develop new therapies for GC, it is necessary to further explore the molecular mechanisms that regulate GC progression.

HOXC9 is a member of the homeobox (HOX) gene family, which contains a homologous domain involved in embryonic development [4]. Recent studies suggest the crucial role of HOXC9 in cancer progression. HOXC9 is highly expressed in glioblastoma and associated with a poor prognosis. HOXC9 silencing activates DAPK1-Beclin1 pathway-induced autophagy in glioblastoma cells, thereby suppressing the proliferation, metastasis, and tumorigenesis of cancer cells [5]. $CD133^+$ glioblastoma cells are tumorigenic stem-like cells. Okamoto et al. showed that HOXC9 is overexpressed in $CD133^+$ glioblastoma cells, suggesting that HOXC9 is involved in the acquisition of stem cell-like phenotype [6]. HOXC9 is highly expressed in breast cancer cells and promotes the switch from a proliferative to an invasive phenotype [7]. However, the role of HOXC9 in GC has not been reported. We analyzed the differential expression profiles of GC tissues and paracancerous tissues using three microarray datasets obtained from the GEO database and found that the HOXC9 gene was significantly upregulated in GC tissues compared with adjacent tissues. The logFC value was 3.92, 3.15, and 4.81, respectively [8-10].

Members of the microRNA (miR)-26 family, including miR-26a and miR-26b, act as tumor suppressor genes and are downregulated in esophageal squamous cancer and hepatocellular carcinoma [11, 12]. A recent study reported that downregulation of miR-26a in GC is indicative of poor prognosis, whereas restoration of miR-26a suppresses the proliferation and metastasis of GC cells [13]. In the present study, the results of bioinformatics analysis identified a conserved binding site for miR-26 (miR-26a/b) in the 3'-untranslated region (3'-UTR) of HOXC9 mRNA, indicating that miR-26 may have an inhibitory effect on HOXC9. However, the interaction remains to be verified.

In the present study, we showed that HOXC9 was overexpressed in GC tissues and promoted the metastasis and stem cell-like phenotype of GC cells. We demonstrated that loss of miR-26a expression led to the upregulation of HOXC9. The present study is the first to demonstrate the role of the miR-26a /HOXC9 axis in the malignant behaviors of GC cells.

Materials and Methods

Gene expression datasets and online survival analysis

Three human GC microarray datasets, GSE103236 (10 patients), GSE79973 (10 patients), and GSE65801 (32 patients) were obtained from the Gene Expression Omnibus (GEO) database (http://www.ncbi.nlm.nih.gov/geo) [14]. Paired GC and adjacent tissues were collected from 52 patients who had undergone radical gastrectomy for GC and did not receive radiotherapy and chemotherapy before surgery. The expression of HOXC9 in GC and matched adjacent tissues was analyzed by GEO2R. The prognostic effect of HOXC9 mRNA in GC was assessed using an online database, Kaplan-Meier Plotter (http://kmplot.com/), which contains gene expression data and survival information of 631 GC patients. Patient samples were divided into a high expression group and a low expression group by auto select best cutoff, and the overall survival (OS) and progression-free survival (PFS) were assessed by a Kaplan-Meier survival plot and the log rank test [15].

Cells and GC specimens.

The human gastric cancer BGC823, MKN45, MKN28, and SGC7901 cell lines were obtained from the Chinese Academy of Sciences Shanghai Cell Bank (Shanghai, China). HEK293 cell line was obtained from the central laboratory of Chongqing Medical University. Cells were cultured in DMEM (Hyclone, Shanghai, China) supplemented with 10% fetal bovine serum (FBS, PAN biotech, Germany) under a humidified

atmosphere containing 5% CO2 at 37°C. 30 pairs of GC tissues and matched non-cancer tissues for qRT-PCR were collected from GC patients admitted to the First Affiliated Hospital of Chongqing Medical University in 2016. TNM staging was as follows: 8 cases of stage I, 10 cases of stage II, 9 cases of stage III, 3 cases of stage IV. For immunohistochemistry analysis, another 95 pairs of GC tissues and matched non-cancer tissues were collected from GC patients admitted to the same hospital between 2011 and 2012. TNM staging was as follows: 30 cases of stage I, 30 cases of stage II, 30 cases of stage III, 5 cases of stage IV. All patients did not undergo radiotherapy and chemotherapy before surgery. The use of human tissue samples and experimental protocols were approved by the Medical Ethics Review Committee of the First Affiliated Hospital of Chongqing Medical University and written informed consent was obtained from all patients.

Immunohistochemistry

Immunohistochemistry was performed on 4-μm-thick paraffin-embedded sections. Antigen retrieval was performed using sodium citrate buffer (pH 6.0), and endogenous peroxidase was blocked with 3% hydrogen peroxide. The slides were incubated with HOXC9 antibody (1:200, Invitrogen, USA) at 4°C overnight. The next day, the slides were incubated with secondary antibody at 37°C for 45 min. Five fields were randomly selected under a light microscope to calculate the percentage of positively stained cells among total cells. The staining range was scored as follows: 0 point, <5%; 1 point, 5%–25%; 2 points, 26%–50%; 3 points, 51%–75%; and 4 points, >75%. The staining intensity was scored as follows: 0 point, no staining; 1 point, light yellow; 2 points, brownish yellow; and 3 points, brown. The final score was the sum of staining range and intensity. A final score of ≤3 points was considered as low expression and ≥4 points was considered as high expression.

Lentiviral transduction

The miR-26a overexpression vector pLV-miR-26a-GFP, the miR-26a silencing vector pLV-anti-miR-26a, the HOXC9 silencing vector pLV-HOXC9-shRNA-GFP, and the negative control vector pLV-NC-GFP were purchased from Hanbio technology (Shanghai, China). The HOXC9-shRNA sequence information was obtained from SIGMA-ALDRICH (www.sigmaaldrich.com) and confirmed by DNAman software (https://www.lynnon.com) to completely match the mRNA of HOXC9, with no binding sites with the downstream genes E-cadherin, N-cadherin, Vimentin, MMP2, MMP9, Twist, Zeb1, Snail, Sox2, Sox4, and Oct4. The shRNA sequences were as follows:

HOXC9-sh1:5'-CCGGGAATCGAAGGATGAAGATGAACTCGAGTTCATCTTCATCCTTCGATTCTTTTTTG-3'
HOXC9-sh2:5'-CCGGCCGGGTTCTCAATCTCACCGACTCGAGTCGGTGAGATTGAGAACCCGGTTTTT-3'
anti-miR-26a:5'-AGCCTATCCTGGATTACTTGAA-3'
NC sequence: 5'-TTCTCCGAACGTGTCACGTAA-3'

Cells were seeded at a density of 2×10^5/ml in six-well plates. The lentiviruses and polybrene (5 μg/ml) were added after cells had adhered to the plate. After 16 h, culture media were changed. The MOI values of BGC823, MKN45, and MKN28 cells were 50, 30, and 30, respectively. Puromycin was added to the cells at a final concentration of 2 μg/ml to select for stable expressing cell lines [16].

Luciferase reporter assay

The miR-26a mimics (5'-TTCAAGTAATCCAGGATAGGCT-3'), dual-luciferase reporter vector, and Lipofectamine 2000 reagent were purchased from Hanbio technology. The 3'-UTR of HOXC9 containing the putative binding sites (5'-TACTTGA-3') was cloned downstream of the luciferase gene to construct a wild-type plasmid (WT). The 3'-UTR containing mutated binding sites (5'-ATGAACT-3') was cloned into the luciferase gene to construct a mutant plasmid (MUT). HEK293 cells were cultured and co-transfected with miR-26a mimics, the WT plasmid, or the MUT plasmid. After 24 h, both firefly and Renilla luciferase activity were detected using a dual-luciferase reporter system (BeyotimeBio, Shanghai, China). The firefly luciferase activity was normalized to the Renilla luciferase activity [17].

Quantitative RT-PCR (qRT-PCR)

Kits for qRT-PCR were purchased from TakaRa (Dalian,China). Primers were purchased from Sangon Biotech (Shanghai, China). Total RNA was extracted using Trizol reagent. Reverse transcription and PCR with SYBR Green for mRNA were performed as described previously [18]. The PCR primers for HOXC9 were as follows: forward: 5'-AGACGCTGGAACTGGAGAAGGAG-3' and reverse: 5'-GCCGCTCGGTGAGATTGAGAAC-3'.

For microRNAs (miRNAs), the stem-loop qRT-PCR was performed to detect the expression. The RT primers were as follows:

miR-26a: 5'-GTCGTATCCAGTGCAGGGTCCGAGGTATTCGCACTGGATACGACAGCCTA-3'

miR-26b: 5'-GTCGTATCCAGTGCAGGGTCCGAGGTATTCGCACTGGATACGACACCTAT-3'

The reverse transcription conditions were as follows: 42°C for 15 min; 85°C for 5 sec.

The PCR primers for miRNAs were as follows:

miR-26a forward: 5'-CGCGTTCAAGTAATCCAGGA-3'

reverse: 5'-AGTGCAGGGTCCGAGGTATT-3'

miR-26b forward: 5'-GCGCGTTCAAGTAATTCAGG-3'

reverse: 5'-AGTGCAGGGTCCGAGGTATT-3'

The PCR conditions were as follows: 95°C for 30 sec; 45 cycles of 95°C for 5 sec; 60°C for 30 sec in a CFX96 real time PCR system (Bio-Rad, USA). GAPDH and U6 snRNA were used as endogenous controls for mRNA and microRNA, respectively. The data were analyzed by the ΔCt [19].

Western blotting

Aliquots containing 25 μg of total protein were separated by sodium dodecyl sulfate-polyacrylamide gel electrophoresis and transferred onto a polyvinylidene fluoride membrane [20]. Different primary antibodies against HOXC9 (1:500, Invitrogen) , E-cadherin (1:1000, Cell Singalling, USA), N-cadherin (1:1000, Cell Singalling), Vimentin (1:2000, Proteintech ,WU Han, China), MMP2 (1:500, Proteintech), MMP7 (1:500, Proteintech), Twist1 (1:500, Proteintech), Zeb1 (1:500, Proteintech), Snail1 (1:1000, Proteintech), SOX2 (1:1000, Santa Cruz, USA), SOX4 (1:1000, Abcam, USA), Oct4 (1:1000, Proteintech), β-catenin (1:1000, Abcam), and GAPDH (1:2000, Proteintech) were added to the samples and incubated at 4°C overnight after non-specific binding was blocked with 5% w/v non-fat milk. Polyvinylidene fluoride membranes were incubated with secondary antibody at 37°C for 2 h. GAPDH was used as the endogenous control. Immunobands were detected using an enhanced chemiluminescence Kit (ECL, Shanghai, China) and the signal intensity was measured by Fusion software (Vilber Lourmat, France) to calculate protein levels. The relative expresson is expressed as the ratio of signal density of the target band to the signal density of the endogenous control.

Immunofluorescence

Adherent cells or cell spheres were permeabilized with 0.25% Triton after fixing with 4% paraformaldehyde for 20 min. Cells or spheres were incubated with different primary antibodies against E-cadherin, N-cadherin, Vimentin, and HOXC9 at 4°C overnight. Cy3-conjugated secondary antibody was incubated at room temperature for 45 min, followed by staining with DAPI for 10 min. Photographs were acquired using a fluorescence microscope.

Transwell assays

Transwell migration and invasion assays were performed as described previously [21]. Briefly, BGC823 or MKN45 cells were seeded at a density of 1×10^5/ml in the upper chamber of a Transwell insert (8 μm pore size) and cultured in 400 μl of medium supplemented with 5% FBS. The bottom chamber was filled with 600 μl of medium supplemented with 10% FBS. After 36 h, metastatic cells were stained and counted under a light microscope.

Cell Counting Kit-8 (*CCK-8*)*, colony-formation, and 5-ethynyl-2'-deoxyuridine (EdU) assays*

For the CCK-8 assay, 2×10^3 cells/well were seeded into 96-well plates (100 μl/well) in quintuplicate, and cultured under conventional conditions. The absorbance was measured at 450 nm after incubating with 10 μl CCK-8 reagent (BeyotimeBio, China) at 37°C for 1 h, and samples were assessed on days 0, 1, 2, and 3. For the colony-formation assay, 500 cells/well were seeded into 24-well plates. After 12 days, cell colonies were stained with crystal violet and counted [21]. For Edu staining, 2×10^3 cells/well were seeded into 96-well plates and cultured for 24 h. Then, cells were incubated with 50 μM EdU for 2 h and DAPI for 15 min at 37°C. Photographs were acquired using a fluorescence microscope to calculate the proliferation rate.

Sphere formation assay

Cells were seeded at a density of 5×10^3/flask into ultra-low attachment flasks and cultured with stem cell medium. A total of 1.5 ml fresh medium was added every 2 days. After 10 days, the number of spheres was counted. Stem cell medium included DMEM/F12 medium + 20 ng/ml bFGF + 10 ng/ml EGF + 2% B27 [22].

Flow cytometry

To detect the percentage of $CD44^+/EpCAM^+$ cells, cells were resuspended in 100 µl buffer. Then, 1 µl of CD44-PE antibody and 0.625 µl of EpCAM-APC antibody were used to stain the antigens at 4°C. After incubation for 20 min, cells were resuspended in 300 µl PBS and analyzed by flow cytometry.

Nude mouse models

The 4-week old nude mice were housed under SPF conditions at Chongqing Medical University. For tumorigenesis assays, 5×10^5 cells were injected subcutaneously into the flanks of each mouse. The tumor volume was calculated as $L\times S^2/2$ (L= the long side, S = the short side) every 3 days. After 30 days, the mice were sacrificed and HOXC9 expression in tumor tissues was detected with immunohistochemistry. For metastasis assays, 1×10^6 cells were injected into the tail veins. After 30 days, the lungs were removed to count the number of nodules [23]. All procedures involving animals were performed in accordance with the guidelines of the National Institutes of Health (NIH) regarding animal care (Department of Health and Human Services, NIH Publication No. 86-23). The animal experimental protocols were approved by the Medical Ethics Review Committee of the First Affiliated Hospital of Chongqing Medical University.

Statistical analysis

All experiments were repeated three times and the data were analyzed using SPSS 19.0. Student's t-test was used for comparisons between two groups. The paired t test was used to analyze the differences of HOXC9 expression between GC tissues and matched tissues of 30 GC patients. The $\chi2$ test was used to analyze the correlation between HOXC9 expression and clinicopathologic parameters. The Kaplan–Meier was used for survival analysis. The correlation between miR-26a and HOXC9 expression was analyzed using Spearman linear regression model. $P<0.05$ was considered statistically significant.

Results

HOXC9 acts as an oncogene that is increased in GC

To determine the expression pattern of HOXC9 in GC, three human GC microarray datasets, namely GSE103236 (10 patients), GSE79973 (10 patients), and GSE65801 (32 patients), were obtained from the GEO database. GC tissues and matched non-cancer tissue were available for the 52 patients, and all patients were diagnosed as primary gastric cancer by postoperative pathological examination [8-10]. The difference in HOXC9 expression between GC tissues and non-cancer tissues were investigated by GEO2R. In GSE103236 (10 patients), GSE79973 (10 patients), and GSE65801 (32 patients), HOXC9 was upregulated in GC tissues by 15.3-, 11.3-, and 28.1-fold, respectively, compared with adjacent tissues in the three datasets (data not shown).

Next, we used qRT-PCR to detect the expression of HOXC9 in 30 GC patients admitted to our hospital and confirmed that HOXC9 mRNA expression was 6.2-fold higher in tumor tissues than that in adjacent non-cancer tissues (Fig. 1A). Immunohistochemistry analysis of another 95 GC samples from the same hospital also detected high HOXC9 expression in 68/95 (71.6%) GC tissues and in 31/95 (32.6%) matched non-cancer tissues, with average staining scores of 4.27 and 2.13, respectively. Further analysis revealed that HOXC9 expression was significantly higher in stage III and IV patients than that in stage I and II patients (5.18 vs. 3.3) (Fig. 1B and C). Increased HOXC9 was significantly correlated with histological grade and TNM stage, but not with age, gender, tumor size, vascular invasion, and distant metastasis (Table 1).

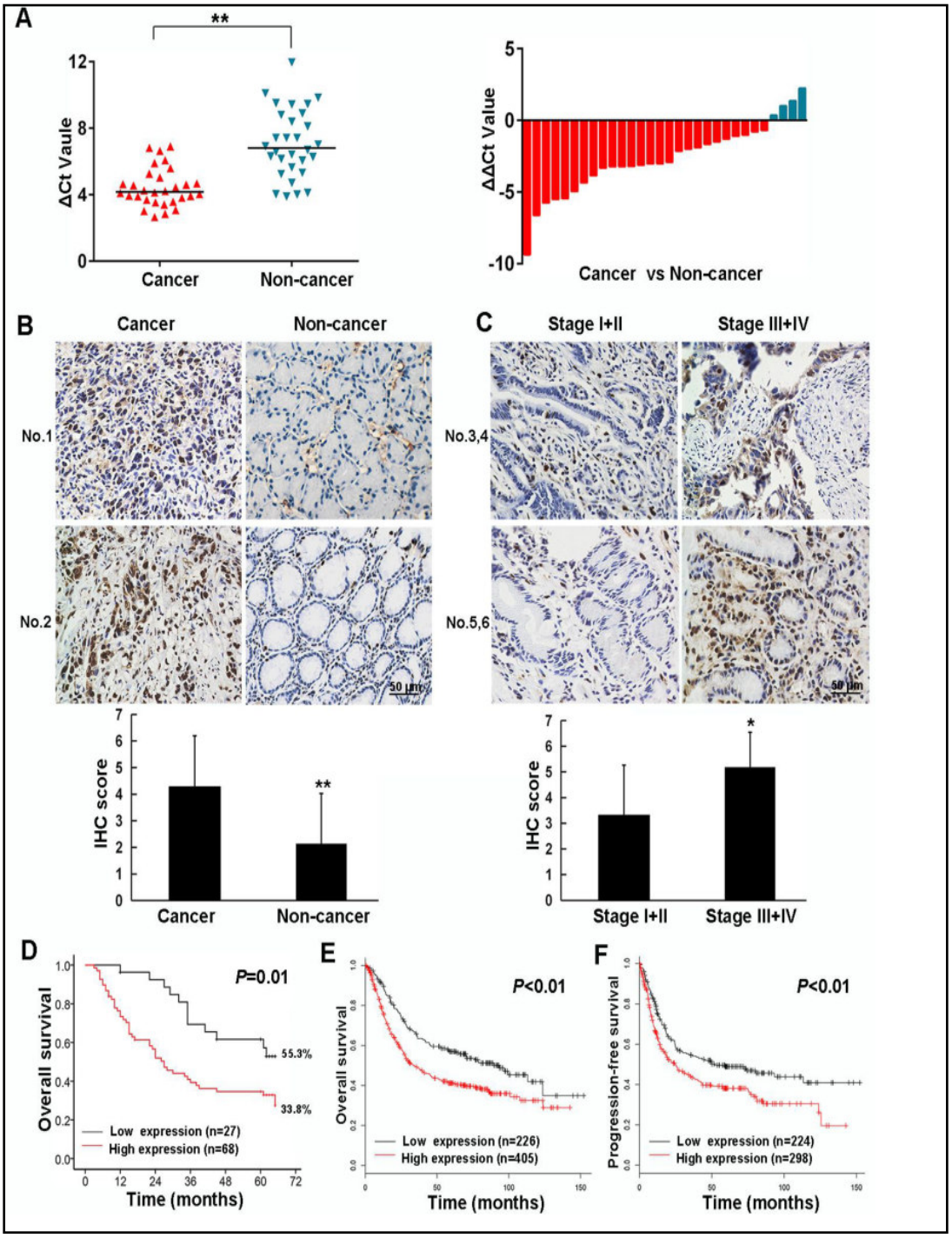

Fig. 1. The expression pattern of HOXC9 in GC tissues. (A) The HOXC9 mRNA in GC and matched non-cancer tissues was detected by qRT-PCR (left). The HOXC9 expression ratio of cancer to non-cancer tissues is expressed as ΔΔCT (right) (n=30). (B) Representative immunohistochemistry staining of HOXC9 and average score in GC and matched non-cancer tissues (n=95). (C) Representative HOXC9 staining and average score of cancer tissues in stage I + II and stage III + IV patients (n=95). (D) Analysis of the overall survival of 95 GC patients admitted to the First Affiliated Hospital of Chongqing Medical University according to HOXC9 immunohistochemistry scores. (E, F) Analysis of of overall survival (E) and progression-free survival (F) of GC patients from the database Kaplan-Meier Plotter according to HOXC9 mRNA expression levels. *P<0.05; **P<0.01.

Furthermore, the correlations of HOXC9 with clinical parameters were analyzed using Kaplan-Meier curves in above 95 GC patients according to the immunohistochemistry score. The 5-year survival rate was 33.8% in patients with high HOXC9 expression and 55.6% in those with low expression. The mean survival time was 51.8 and 34.2 months, respectively (Fig. 1D). Multivariate analysis revealed that similar to tumor size, TNM stage, and distant metastasis, HOXC9 upregulation was an independent prognostic factor for overall survival (Table 2). Information from the database Kaplan-Meier Plotter also confirmed patients with high HOXC9 expression had shorter overall survival (OS) and progression free survival (PFS) than those with low expression (Fig. 1E and F). These results suggest that HOXC9 is upregulated in GC and indicates a poor prognosis.

Table 1. Correlation between HOXC9 and clinical parameters of GC patients

Index		HOXC9			
	Case	-	+	χ2	P
Sex				0.033	0.856
Female	33	9	24		
Male	62	18	44		
Age (years)				0.246	0.62
<60	35	11	24		
≥60	60	16	44		
Histological grade				7.483	0.006**
Poorly differentiated	39	17	22		
Well differentiated	56	10	46		
Tumor size				0.891	0.345
<5cm	49	16	33		
≥5cm	46	11	35		
TNM stage				5.028	0.025*
1+2	46	18	28		
3+4	49	9	40		
Vascular invasion				2.523	0.112
Absent	64	18	46		
Present	31	9	22		
Distant metastasis				0.006	0.936
No	90	25	65		
Yes	5	2	3		

Table 2. Kaplan-Meier univariate survival analysis and multivariate analysis of prognostic factors in GC for overall survival

Variables	Univariate analysis	Multivariate analysis		
	P	HR	95%CI	P
Sex	0.672			
Age	0.507			
Histological grade	0.179	1.5	0.844-2.63	0.167
Tumor size	<0.001**	2.454	1.387-4.341	0.002**
TNM stage	<0.001**	2.082	1.103-3.929	0.024*
Vascular invasion	0.084	0.996	0.544-1.823	0.989
Distant metastasis	<0.001**	4.716	1.610-13.814	0.002**
HOXC9 expression	0.01*	2.248	1.0684 -4.734	0.033*

HOXC9 has no effect on the proliferation of GC cells

Loss of controlled cell proliferation is one of the important characteristics of cancer cells. To determine whether HOXC9 promoted GC progression by affecting the regulation of cell proliferation, the GC cell lines BGC823 and MKN45 were transduced with lentiviral vector expressing HOXC9 shRNA to knock down HOXC9 (Fig. 2A). Compared with HOXC9-sh1, HOXC9-sh2 revealed a better knock-down effect on HOXC9 mRNA in BGC823 cells (knockdown efficiency*:* 88.6% vs 68.7%) and MKN45 cells (knockdown efficiency*:* 76.8% vs 62.3%) (data not shown), and it was therefore selected as the target sequence for subsequent experiments. The CCK-8 growth curve showed no significant changes in the proliferation of GC cells in response to HOXC9 silencing. The colony formation assay showed that the colony-forming ability did not differ between the HOXC9 knockdown cell lines BGC823-sh and MKN45-sh and negative control cells (NC) (Fig. 2B). Staining of proliferative cells with Edu showed that HOXC9 knockdown had no effect on the proliferation index of BGC823 and MKN45 cells (Fig. 2C). Taken together, these results suggested that HOXC9 has no effect on the proliferation of GC cells.

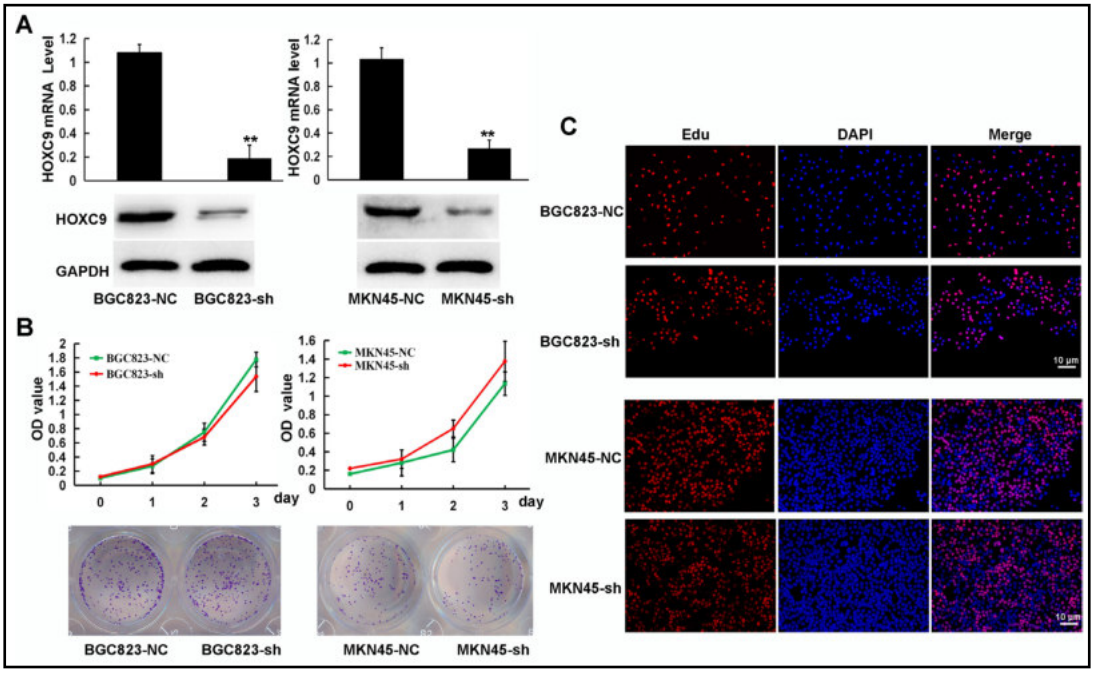

Fig. 2. The effect of HOXC9 on GC cell proliferation. (A) BGC823 and MKN45 cells were transduced with lentiviral vector expressing HOXC9 shRNA (sh) and negative control shRNA (NC). Knockdown efficiency was detected with qRT-PCR and western blotting. (B) The CCK-8 growth curve (higher) and colony-formation assay (lower) were used to investigate the effect of HOXC9 knockdown on proliferation. (C) Cells were seeded in 96-well plates and stained with EdU and DAPI. The proliferation index was calculated using EdU-stained cell (red) number compared with DAPI-stained cell number (blue). n=3, **P<0.01 vs. BGC823-NC group.

HOXC9 knockdown suppresses the metastasis of GC cells

The correlation between HOXC9 expression and GC TNM stage indicated that HOXC9 may play a role in the migration and invasion of GC cells. To verify this hypothesis, Transwell assays were performed using BGC823 and MKN45 cells transduced with HOXC9-shRNA or NC-shRNA. The results showed that HOXC9 silencing significantly reduced the numbers of migrated and invaded BGC823 and MKN45 cells (Fig. 3A).

Matrix metalloproteinases (MMPs) play a crucial role in the degradation of extracellular matrix proteins, thereby promoting cell metastasis. Assessment of MMP2 and MMP9 expression showed that MMP2 was significantly downregulated following HOXC9 knockdown in BGC823 and MKN45 cells, whereas MMP9 expression did not change significantly. EMT is a pivotal process for the acquisition of metastatic potential in cancer cells. We therefore detected the expression of EMT markers with western blotting and immunofluorescence. The expression of the mesenchymal markers N-cadherin and vimentin was significantly lower in BGC823-sh cells than in BGC823-NC cells, whereas no changes in the expression of the epithelial marker E-cadherin were observed. Silencing HOXC9 downregulated N-cadherin and upregulated E-cadherin in MKN45 cells (Fig. 3B and C).

HOXC9 is required for GC cell stem cell-like phenotype

HOXC9 was previously shown to enhance the self-renewal and tumorigenesis of glioma cells [5]. To investigate whether HOXC9 also promoted the stem cell-like phenotypic acquisition of GC cells, we transduced BGC823 and MKN45 cells with lentiviral vector expressing HOXC9-shRNA or NC-shRNA at a MOI of 50 and 30, respectively. Flow cytometry was used to examine the percentage of $CD44^+/EpCAM^+$ GC cells, which were reported to possess stem cell-like properties. The percentage of $CD44^+/EpCAM^+$ cells in the BGC823-sh group decreased from 35.6% to 10.6% and from 14.4% to 5.3% in the MKN45-sh group

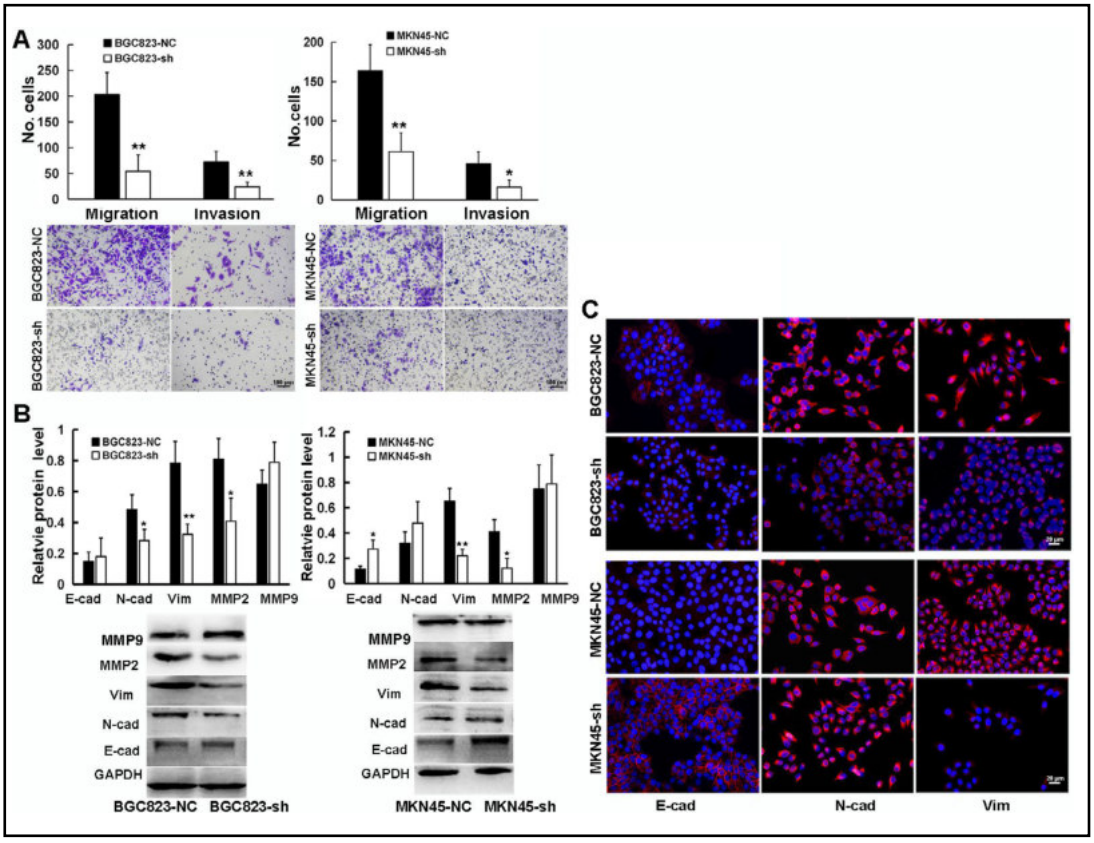

Fig. 3. HOXC9 knockdown suppresses the metastatic capacity of GC cells. BGC823 and MKN45 cells transfected with HOXC9-shRNA (sh) or negative control shRNA (NC) vector were used in the following experiments. (A) The metastatic capability was detected by Transwell migration and invasion assays. After incubation for 36 h in plates with Transwell inserts, metastatic cells was stained and counted. (B) Five metastasis associated molecules were detected by western blotting. GAPDH was used as the endogenous control. (C) Immunofluorescence was performed to evaluate the expression of E-cadherin, N-cadherin, and vimentin in GC cells. n=3, *P<0.05; **P<0.01 vs. NC group.

compared with the NC group (Fig. 4A). Next,the effect of HOXC9 on self-renewal was examined by sphere formation assays. 10 days later, the number of spheres decreased by 72% and 69.4% in BGC823 and MKN45 cells, respectively. Consistently, compared with the control vector, transduction with HOXC9-sh vector also significantly decreased the size of spheres in GC cells (Fig. 4A). These results confirmed the effect of HOXC9 on promoting stem cell-like phenotype in GC cells.

Furthermore, the sphere formation assay was used to enrich cancer stem cells (CSCs) in SGC7901 cells which have low HOXC9 expression, and the difference in HOXC9 expression between differentiated GC cells and GC stem cells was examined using immunofluorescence and western blotting. As shown in Fig. 4B and C, compared with adherent cells (SGC7901-A), the HOXC9 protein expression level in SGC7901 spheres (SGC7901-S) were significantly increased. These data indicated that HOXC9 is overexpressed in CSCs from GC compared with non-CSCs, which further suggested that HOXC9 promotes GC stem cell-like properties.

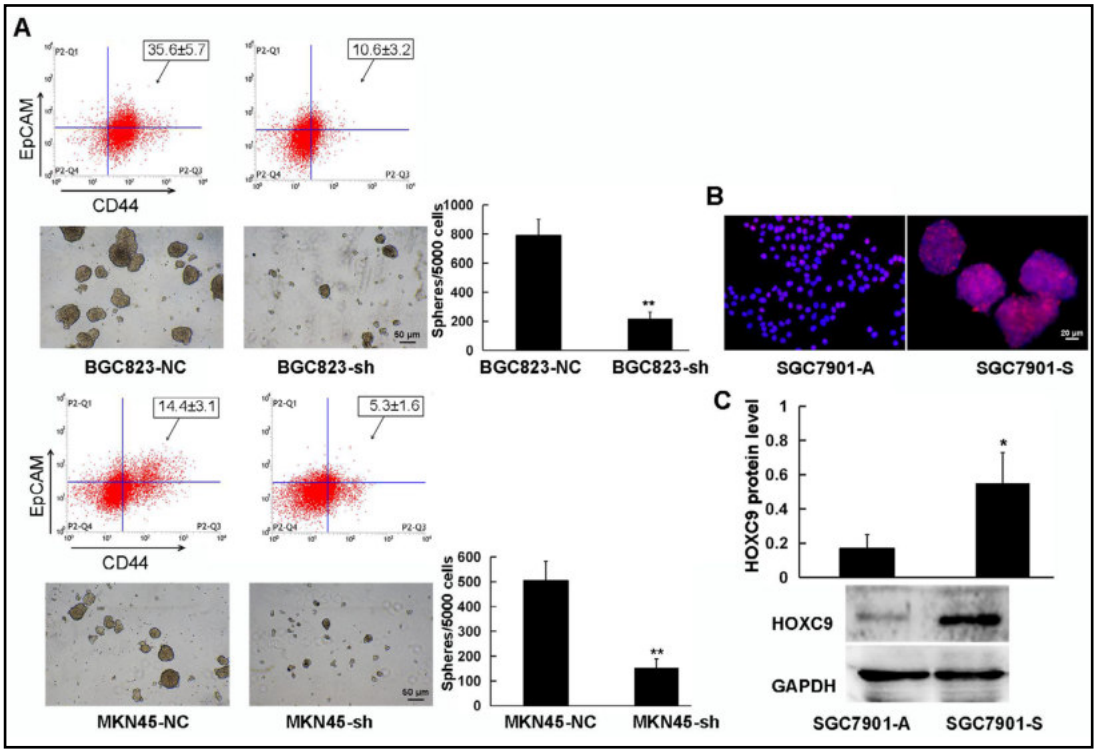

Fig. 4. HOXC9 knockdown suppresses the stem cell-like phenotype of GC cells. (A) BGC823 and MKN45 cells were transduced with lentiviral vector expressing HOXC9 shRNA (sh) or negative control shRNA (NC), and the percentage of $CD44^+/EpCAM^+$ cells was determined with flow cytometry and the self-renewal was assessed using a sphere formation assay. n=3, **P<0.01 vs. NC group. (B, C) CSCs in SGC7901 cells were enriched by the sphere formation assay. The protein expression of adherent SGC7901 cells (SGC7901-A) and SGC7901 spheres (SGC7901-S) were assessed using immunofluorescence and western blotting. n=3, *P<0.05 vs. SGC7901-A group.

HOXC9 upregulates transcription factors to promote metastasis and stem cell-like phenotype

To assess whether HOXC9 activates Wnt signaling, which plays a crucial role on metastasis and self-renewal, we used western blotting and immunofluorescence to detect the total expression and localization of β-catenin after HOXC9 knockdown. We found that HOXC9 silencing in BGC823 and MKN45 cells did not decrease β-catenin total expression and nuclear staining (Fig. 5A and B).

To further determine the mechanism by which HOXC9 promotes metastasis and stem cell-like phenotype in GC, the expression of EMT-associated transcription factors (Twist1, Snail1, and Zeb1) and stemness-associated transcription factors (SOX2, SOX4, and Oct4) was assessed by western blotting in HOXC9 knockdown cells. HOXC9 silencing downregulated Twist1, Zeb1, and SOX2 in BGC823 cells and downregulated Twist1, Snail1, and SOX2 in MKN45 cells (Fig. 5C). These results indicated that HOXC9 may function through specific transcription factors to promote metastasis and stem cell-like phenotype in GC cells.

miR-26a is a negative regulator of HOXC9

To examine the regulatory mechanisms underlying the upregulation of HOXC9 in GC, candidate upstream miRNAs were predicted using three databases: TargetScan, miRanda, and Microcosm. miR-26 (miR-26a/b), a tumor suppressor miRNA, was consistently predicted to bind the 3′-UTR of HOXC9 mRNA (Fig. 6A). In view of the high conservation and low mirSVR score, we speculated that the binding site is a functional site. The qRT-PCR results showed that miR-26a expression was 5.2-fold lower in GC than in non-tumor tissues, whereas miR-26b showed no significant difference (Fig. 6B). Contrary to the HOXC9 expression pattern,

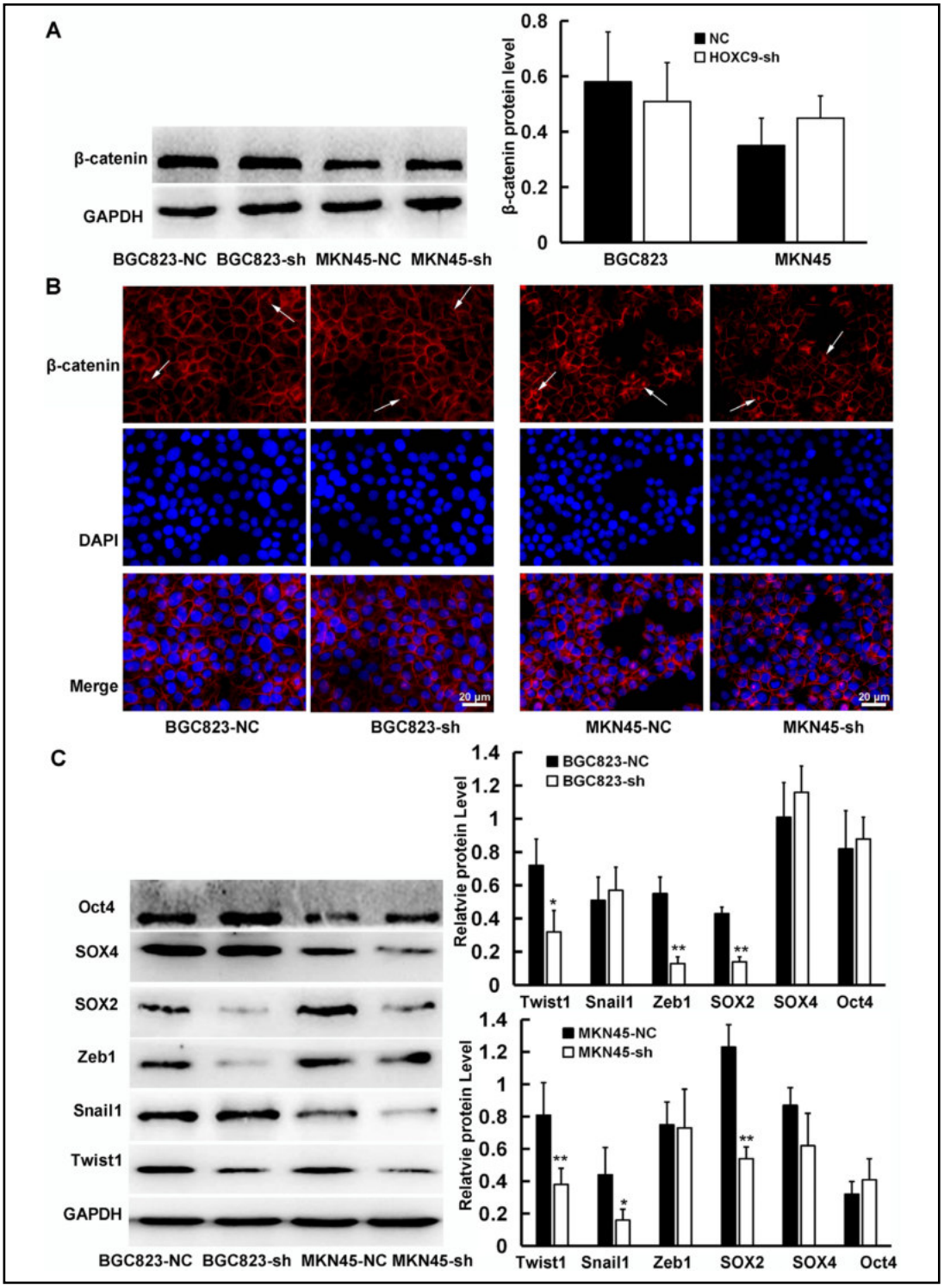

Fig. 5. HOXC9 silencing downregulates EMT/stemness-associated transcription factors, but not Wnt signaling. (A) BGC823 and MKN45 cells were transduced with HOXC9 shRNA (sh) or negative control shRNA (NC) vector. The total protein of β-catenin was determined by western blotting. (B) Cells were treated as A, and immunofluorescence analysis of β-catenin was performed. DAPI was used to stain nucleus. (C) The expression of Oct4, SOX4, SOX2, Twist1, Snail1 and Zeb1 was detected by western blotting. n=3, *P<0.05; **P<0.01 vs. NC group.

miR-26a expression in stage III and IV patients was 2.1 times lower than that in stage I and II patients. Further analysis revealed an inverse correlation between miR-26a and HOXC9 at the mRNA level (Fig. 6C).

Given that the BGC823 cell line has low miR-26a expression, whereas the MKN28 cell line expresses high levels of miR-26a, we examined the regulatory effect of miR-26a on HOXC9. Lentiviral vectors were used to stably restore or knock down miR-26a in BGC823 and MKN28 cells. HOXC9 expression was decreased by 78.3% at the mRNA level and 65.3% at the protein level in BGC823 cells after miR-26a restoration. Contrasting results were obtained in MKN28 with miR-26a knockdown (Fig. 6D). The results of dual-luciferase reporter assay showed that miR-26a greatly decreased the luciferase activity of the WT vector containing the predicted binding sites but not the MUT vector containing mutated sites in HEK293 cells compared with the NC group, which indicated that miR-26a can directly bind to the 3′-UTR of HOXC9 mRNA (Fig. 6E). These data strongly indicated that miR-26a is a negative regulator of HOXC9.

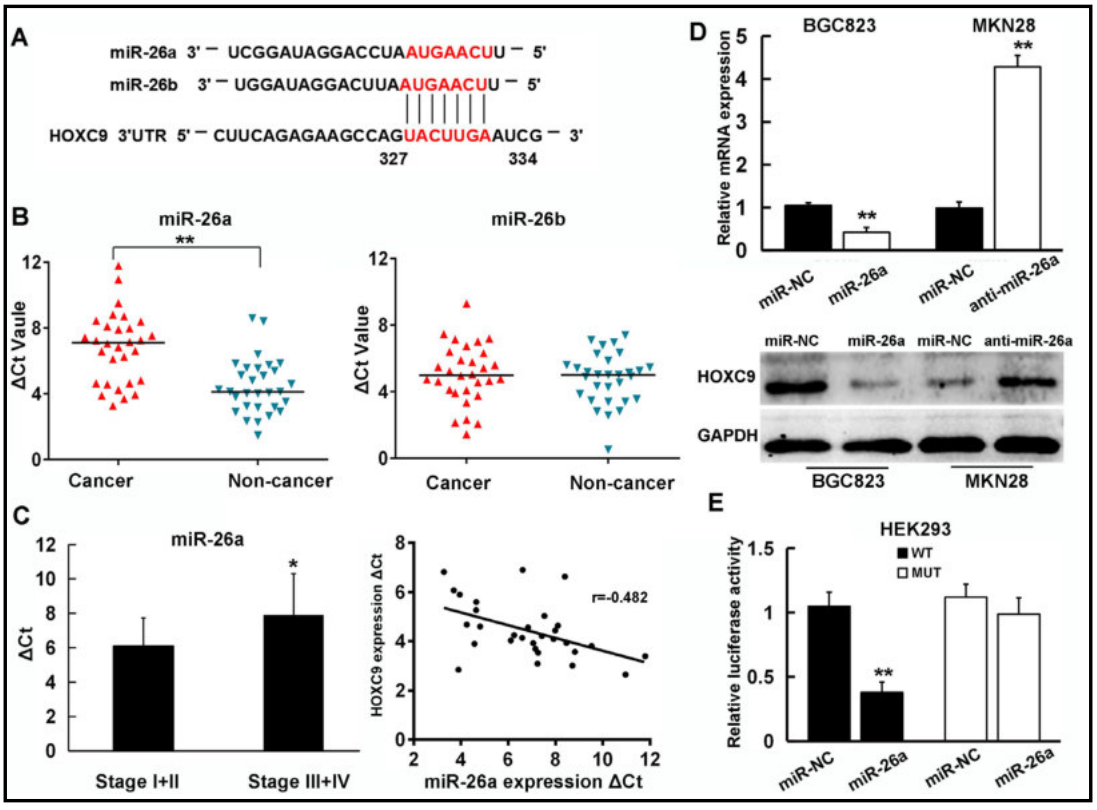

Fig. 6. miR-26a is a negative regulator of HOXC9. (A) Predicted binding site between miR-26a/b and the 3′-UTR of HOXC9 mRNA. (B) miR-26a/b expression in cancer and matched non-cancer tissues was detected with qRT-PCR (n=30). (C) miR-26a expression in stage I + II and stage III + IV GC patients and its correlation with HOXC9 mRNA were analyzed. Higher ΔCt values indicate lower expression. (D) BGC823 and MKN28 cells were transduced with miR-26a overexpression vector, knockdown vector (anti-miR-26a) or negative control (miR-NC) vector. HOXC9 was detected using qRT-PCR and western blotting. (E) HEK293 cells were cotransfected with wild-type (WT) or mutant plasmid (MUT) vectors and miR-26a mimics or negative control (miR-NC). After 24 h, luciferase activity was detected using a dual-luciferase reporter system. n=3, *P<0.05; **P<0.01 vs. NC group.

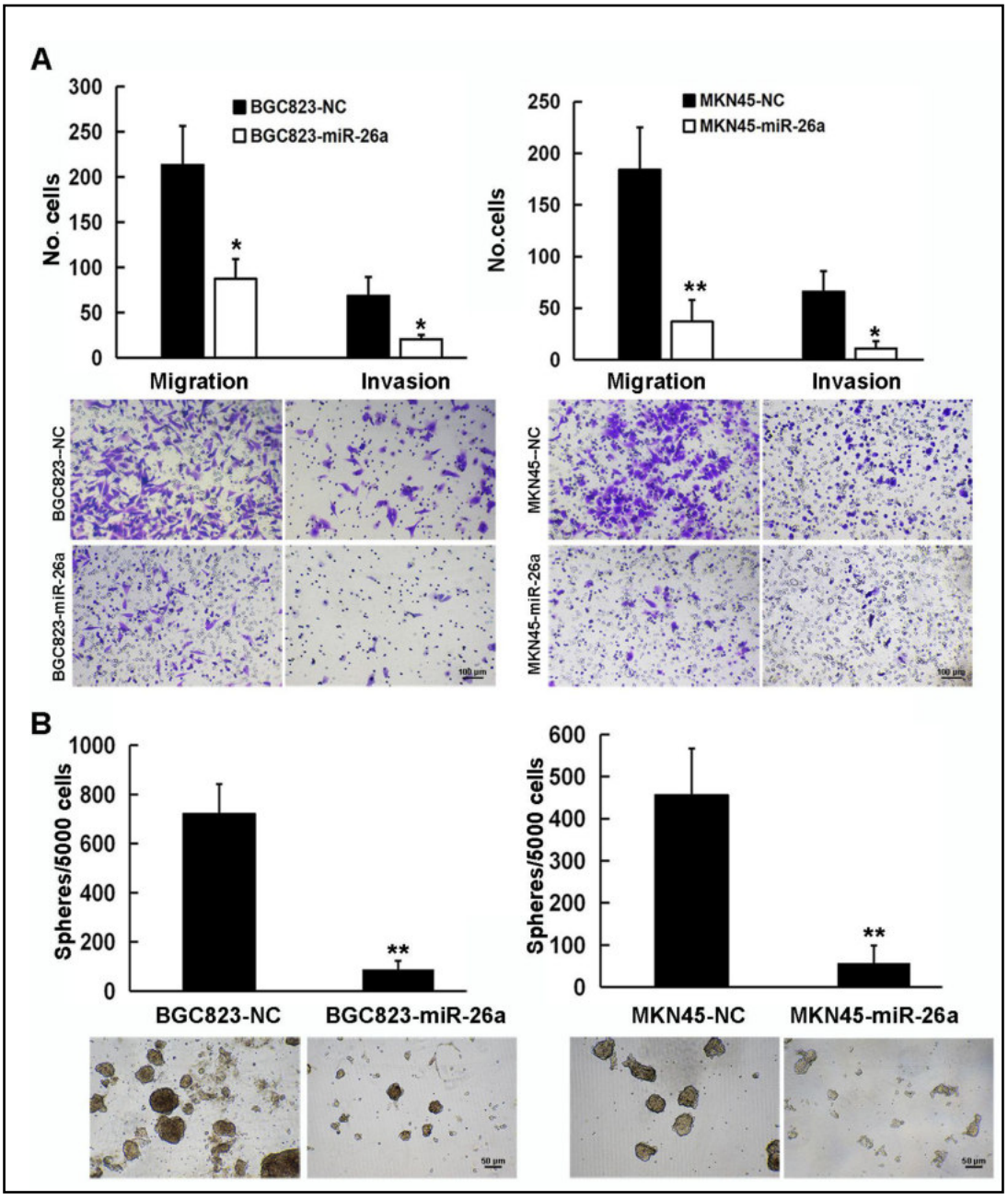

Fig. 7. Restoration of miR-26a suppressed HOXC9 mediated malignant behaviors of GC cells. (A) The metastatic capability of BGC823 (left) and MKN45 (right) cells transfected with miR-26a or negative control (NC) vector was detected with Transwell assays. (B) The self-renewal was assessed with sphere formation assay after miR-26a was restored in BGC823 (left) and MKN45 cells (right). n=3, *P<0.05; **P<0.01 vs. NC group.

miR-26a restoration suppresses metastasis and stem cell-like phenotype through the miR-26a/HOXC9 axis

The results showing that miR-26a targets HOXC9 mRNA and suppresses its expression led us to investigate whether miR-26a can inhibit GC malignant behaviors through the regulation of HOXC9. We used a lentiviral vector to stably restore miR-26a expression in BGC823 and MKN45 cells (data not shown). Restoration of miR-26a expression in GC cells

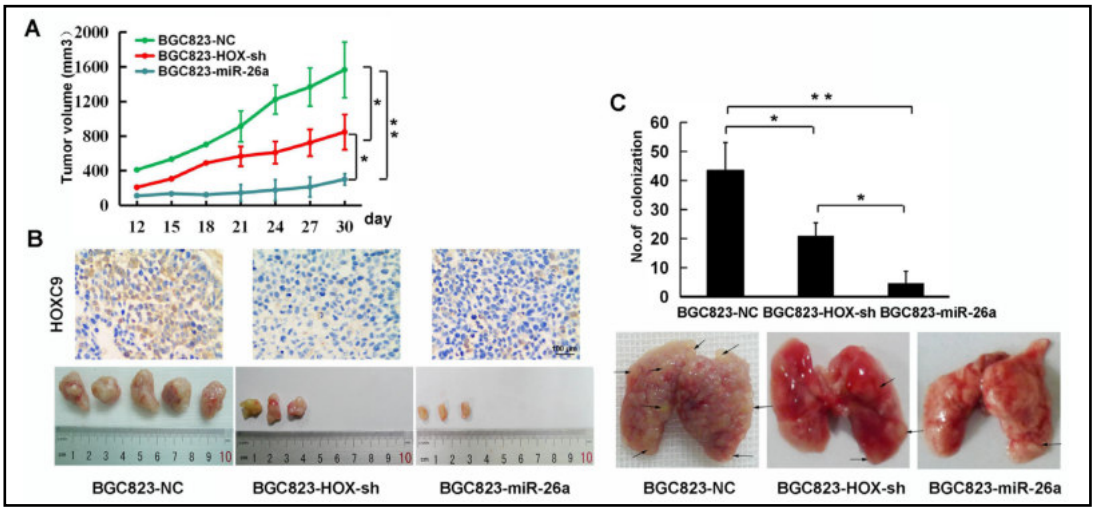

Fig. 8. In vivo assessment of the miR-26a/HOXC9 axis in tumorigenesis and metastasis of GC cells. (A) BGC823 cells (5×10^5) transfected with lentiviruses carrying negative control (NC) sequences, HOXC9 shRNA (HOX-sh), or miR-26a were subcutaneously injected into nude mice. After 30 days, tumor samples were collected, and the final volume was measured and analyzed. (B) Immunohistochemistry was performed to analyze the protein expression of HOXC9. (C) BGC823-NC, BGC823-HOX-sh, and BGC823-miR-26a cells were injected into the tail veins of mice. After 30 days, the lungs were removed to count the nodule number. n=3, *P<0.05; **P<0.01.

decreased the metastatic capacity, as shown by Transwell assays (Fig. 7A). Sphere formation assays revealed that forced miR-26a restoration suppressed the self-renewal of GC cells (Fig. 7B). Taken together, these data indicate that miR-26a may function as a tumor suppressor gene and form a miR-26a/HOXC9 axis involved in GC metastasis and stem cell-like phenotype.

HOXC9 promotes tumorigenesis and metastasis of GC cells in vivo, and the effect is reversed by miR-26a

Finally, we investigated the functional role of the miR-26a/HOXC9 axis in tumorigenesis. Three stable cell lines transfected with lentiviruses carrying NC sequences (BGC823-NC), HOXC9 shRNA (BGC823-HOX-sh), or miR-26a (BGC823-miR-26a) were subcutaneously injected into nude mice to examine the tumorigenic capacity. In the group injected with BGC823-NC cells, all five mice (5/5) developed subcutaneous tumors, whereas two mice (2/5) injected with BGC823-HOX-sh cells developed tumors. Although *in vitro* experiments did not show the effect of HOXC9 on the proliferation of GC cells, the tumors in the BGC823-sh group were smaller than those in the BGC823-NC group. Tumors in the BGC823-miR-26a group showed a lower formation rate and slower growth than those in the BGC823-NC group (Fig. 8A). The results of immunohistochemistry showed that HOXC9 protein expression was significantly lower in the BGC823-HOX-sh and BGC823-miR-26a groups than in the BGC823-NC group (Fig. 8B).

We performed intravenous injection through the tail vein with the same cells to investigate the role of the miR-26a/HOXC9 axis on metastasis. After 6 weeks, there were fewer lung metastatic nodules in the BGC823-HOX-sh and BGC823-miR-26a groups than in the BGC823-NC group. The BGC823-miR-26a group exhibited weaker proliferative and metastatic potentials than the BGC823-HOX-sh group (Fig. 8C).

Discussion

The functional role of HOXC9 in GC has not been reported to date. Herein, we showed that HOXC9 acts as an oncogene and elucidated the involvement of the miR-26a/HOXC9 axis in GC.

The homeobox gene family (HOX) comprises four clusters: HOXA, HOXB, HOXC, and HOXD. All HOX members contain a highly conserved sequence consisting of 180–183 bases. The sequence encodes a polypeptide region called the homologous domain (homeodomain, HD). HOXC9 is located in human chromosome 12q13.13. Previous studies provided evidence that HOXC9 is involved in the progression of glioblastoma and breast cancer. In this study, we confirmed that HOXC9 is upregulated in GC tissues compared with matched non-cancer tissues, which was consistent with the expression profile obtained from three GEO data sets including 54 GC patients. Specifically, HOXC9 expression was higher in stage III and IV patients than in early stage patients. Further analysis showed that HOXC9 upregulation in GC tissues suggested that the tumor was poorly differentiated and associated with a late TNM stage. The Kaplan–Meier curve combined with Cox analysis revealed that HOXC9 overexpression was correlated with a poor prognosis in GC patients.

The malignant characteristics of GC cells include aberrant proliferation, enhanced angiogenesis, metastasis, and so on. Recently, stem cell-like phenotype, an unstable cell phenotype, is also an important malignant behavior of cancer cells, leading to tumor progression. To further explore the mechanism by which HOXC9 promoted GC progression, we knocked down the expression of HOXC9 in GC cell lines using a lentiviral vector expressing shRNA to determine the effect of HOXC9 on proliferation, metastasis, and stem cell-like phenotype. Although the data showed no effect on cell proliferation, HOXC9 knockdown inhibited invasion and reduced the self-renewal ability and the percentage of $CD44^+/EpCAM^+$ cells, which were considered to possess the properties of CSCs. This result is consistent with the finding by Hur et al. that HOXC9 induces phenotypic switching between proliferation and invasion in breast cancer cell and the finding by Xuan et al. that HOXC9 promotes self-renewal of glioblastoma cells [5, 7].

The Wnt/β-cantenin pathway is closely related to EMT and self-renewal of GC cells [24]. Previous studies showed that certain transcription factors stabilize β-catenin by modulating APC or CK2 or by promoting β-catenin nuclear translocation by direct binding to β-catenin, thereby enhancing the activity of the β-catenin/TCF complex and Wnt pathway [25, 26]. In the present study, we also explored whether HOXC9 can activate the Wnt pathway. However, our results suggested that HOXC9 has no effect on the Wnt pathway. Multiple transcription factors are involved in the regulation of tumor metastasis and stem cell-like phenotype. The EMT-associated transcription factors Snail, ZEB, and Twist promote EMT by regulating E-cadherin, N-cadherin, and Vimentin, thereby enhancing the metastatic ability of GC cells. The stemness-associated transcription factors Oct4, SOX2, and SOX4 can regulate the transcription of genes required for the maintenance of the self-renewal, thereby promoting the stem cell-like characteristics of cancer cells. Here, we found that HOXC9 knockdown suppressed the expression of the EMT-associated transcription factors Twist1, Snail1, and Zeb1 and the expression of the stemness-associated transcription factor SOX2, which indicates that HOXC9 facilitates the EMT and stem cell-like phenotype of GC cells through the regulation of EMT/stemness-associated transcription factors.

miRNAs, as a type of non-coding RNAs, are involved in cellular processes such as proliferation, apoptosis, and embryonic development [27]. miRNAs function as oncogenes or tumor suppressor genes in cancer by modulating the translation and stability of target mRNAs [28, 29]. We used bioinformatics methods to identify a conserved miR-26 binding site in the 3'-UTR of HOXC9 mRNA. Since miR-26a, a miR-26 family member, was downregulated in GC, we suspected that the loss of miR-26a expression leads to HOXC9 upregulation in GC [12]. The present results suggest the presence of a miR-26a/HOXC9 axis in GC. To confirm this hypothesis, miR-26a/b expression was detected. In contrast to the pattern of HOXC9 expression, miR-26a, but not miR-26b, was downregulated in GC tissues compared with

non-cancer tissues. Furthermore, miR-26a expression was lower in patients with advanced GC than in early-stage patients. Subsequent functional experiments demonstrated that miR-26a can target the 3'-UTR of HOXC9 mRNA, promoting the degradation of HOXC9. miR-26 inhibits proliferation and enhances chemosensitivity and apoptosis in esophageal cancer and hepatocellular carcinoma. However, the function of miR-26a in GC has not been reported to date. In view of the effect of HOXC9 on metastasis and stem cell-like phenotypic acquisition, we examined whether miR-26a can also inhibit GC cell metastasis and stem cell-like characteristics. miR-26a restoration reduced the number of migrated and invaded cells, and decreased the self-renewal capacity of stem-like cells. These data confirmed that miR-26a can inhibit HOXC9 mediated GC metastasis and stem cell-like phenotype of GC cells, which indicates the presence of a miR-26a/HOXC9 axis.

Finally, we assessed the functional role of the miR-26a/HOXC9 axis in nude mice. Consistent with the *in vitro* experiments, HOXC9 knockdown inhibited tumorigenesis and lung colonization of GC cells, and this effect was mimicked by miR-26a restoration. Although HOXC9 had no effect on the proliferation of GC cells *in vitro*, experiments *in vivo* demonstrated that HOXC9 knockdown inhibited the growth of xenografts. In the *in vivo* microenvironment, CSCs are the source of tumor growth [30, 31]. We speculated that the reduction of CSCs induced by HOXC9 knockdown in tumors resulted in decreased tumor proliferation. Although miR-26a may exert its anti-cancer effect through the negative regulation of HOXC9, we found that miR-26a restoration inhibited tumor proliferation and metastasis to a greater extent than HOXC9 knockdown. One possible explanation is that the functional effects of miR-26a on malignant behaviors may be executed through other targets. Theoretically, a microRNA can target tens or hundreds of mRNAs. Therefore, the suppression of other targets such as c-Myc or EZH2 may contribute to the anti-cancer effect of miR-26a in GC [11, 23].

Taken together, the present results indicated that HOXC9 promotes the metastasis and stem cell-like phenotypic acquisition of GC cells through EMT or stemness-associated transcription factors. In addition, loss of miR-26a may be a crucial factor leading to the abnormal overexpression of HOXC9 in GC. Restoring miR-26a suppressed HOXC9 expression in GC cells and reversed its tumor-promoting effect. The present study identified the role of the miR-26a/HOXC9 axis in GC metastasis and stem cell-like phenotype and may provide a potential therapeutic target for the treatment of GC.

Conclusion

In summary, our research demonstrated for the first time that HOXC9 acted as a driver gene in GC metastasis and stem cell-like phenotype by regulating EMT and stemness-associated transcription factors expression. In addition, we showed that miR-26a can inhibit the promoting effect of metastasis and stem cell-like phenotype, suggesting the presence of a miR-26a/HOXC9 axis in GC. These findings provide further insight into the cancer biology of GC and suggest that miR-26a and HOXC9 are potential therapeutic targets for the development of therapies for GC.

Acknowledgements

This study was supported by National Key Clinical Specialties Construction Program of China (No [2012].649). We thank *International Science Editing* (http://www.internationalscienceediting.com) for editing this manuscript.

Disclosure Statement

The authors declare no conflicts of interest.

References

1 Torre LA, Bray F, Siegel RL, Ferlay J, Lortet-Tieulent J, Jemal A: Global cancer statistics, 2012. CA Cancer J Clin 2015;65:87-108.
2 Fuchs CS, Tomasek J, Yong CJ, Dumitru F, Passalacqua R, Goswami C, Safran H, Dos Santos LV, Aprile G, Ferry DR, Melichar B, Tehfe M, Topuzov E, Zalcberg JR, Chau I, Campbell W, Sivanandan C, Pikiel J, Koshiji M, Hsu Y et al.: Ramucirumab monotherapy for previously treated advanced gastric or gastro-oesophageal junction adenocarcinoma (REGARD): an international, randomised, multicentre, placebo-controlled, phase 3 trial. Lancet 2014;383:31-39.
3 Okines AF, Dewdney A, Chau I, Rao S, Cunningham D: Trastuzumab for gastric cancer treatment. Lancet 2010;376:1736; author reply 1736-1737.
4 Mark M, Rijli FM, Chambon P: Homeobox genes in embryogenesis and pathogenesis. Pediatr Res 1997;42:421-429.
5 Xuan F, Huang M, Liu W, Ding H, Yang L, Cui H: Homeobox C9 suppresses Beclin1-mediated autophagy in glioblastoma by directly inhibiting the transcription of death-associated protein kinase 1. Neuro Oncol 2016;18:819-829.
6 Okamoto OK, Oba-Shinjo SM, Lopes L, Nagahashi Marie SK: Expression of HOXC9 and E2F2 are up-regulated in CD133(+) cells isolated from human astrocytomas and associate with transformation of human astrocytes. Biochim Biophys Acta 2007;1769:437-442.
7 Hur H, Lee J, Yang S, Kim J, Park A, Kim M: HOXC9 Induces Phenotypic Switching between Proliferation and Invasion in Breast Cancer Cells. J Cancer 2016;7:768-773.
8 Chivu Economescu M, Necula L, Dragu D, Badea L, Dima S, Tudor S, Nastase A, Popescu I, Diaconu C: Identification of potential biomarkers for early and advanced gastric adenocarcinoma detection. Hepatogastroenterology 2010;57:1453-1464.
9 He J, Jin Y, Chen Y, Yao H, Xia Y, Ma Y, Wang W, Shao Q: Downregulation of ALDOB is associated with poor prognosis of patients with gastric cancer. Onco Targets Ther 2016;9:6099-6109.
10 Li H, Yu B, Li J, Su L, Yan M, Zhang J, Li C, Zhu Z, Liu B: Characterization of differentially expressed genes involved in pathways associated with gastric cancer. PLoS One 2015;10:e0125013.
11 Li J, Liang Y, Lv H, Meng H, Xiong G, Guan X, Chen X, Bai Y, Wang K: miR-26a and miR-26b inhibit esophageal squamous cancer cell proliferation through suppression of c-MYC pathway. Gene 2017;625:1-9.
12 Qiu X, Zhu H, Liu S, Tao G, Jin J, Chu H, Wang M, Tong N, Gong W, Zhao Q, Qiang F, Zhang Z: Expression and prognostic value of microRNA-26a and microRNA-148a in gastric cancer. J Gastroenterol Hepatol 2017;32:819-827.
13 Jin F, Wang Y, Li M, Zhu Y, Liang H, Wang C, Wang F, Zhang C, Zen K, Li L: MiR-26 enhances chemosensitivity and promotes apoptosis of hepatocellular carcinoma cells through inhibiting autophagy. Cell Death Dis 2017;8:e2540.
14 Zhu Q, Lv T, Wu Y, Shi X, Liu H, Song Y: Long non-coding RNA 00312 regulated by HOXA5 inhibits tumour proliferation and promotes apoptosis in Non-small cell lung cancer. J Cell Mol Med 2017;21:2184-2198.
15 Szász A, Lánczky A, Nagy Á, Förster S, Hark K, Green J, Boussioutas A, Busuttil R, Szabó A, Győrffy B: Cross-validation of survival associated biomarkers in gastric cancer using transcriptomic data of 1, 065 patients. Oncotarget 2016;7:49322-49333.
16 Qiao Y, Jiang X, Lee S, Karuturi R, Hooi S, Yu Q: FOXQ1 regulates epithelial-mesenchymal transition in human cancers. Cancer Res 2011;71:3076-3086.
17 Wu J, Liu Z, Shao C, Gong Y, Hernando E, Lee P, Narita M, Muller W, Liu J, Wei J: HMGA2 overexpression-induced ovarian surface epithelial transformation is mediated through regulation of EMT genes. Cancer Res 2011;71:349-359.
18 Peng X, Luo Z, Kang Q, Deng D, Wang Q, Peng H, Wang S, Wei Z: FOXQ1 mediates the crosstalk between TGF-β and Wnt signaling pathways in the progression of colorectal cancer. Cancer Biol Ther 2015;16:1099-1109.
19 Livak K, Schmittgen T: Analysis of relative gene expression data using real-time quantitative PCR and the 2(-Delta Delta C(T)) Method. Methods 2001;25:402-408.
20 Yeh T, Lin Y, Hsieh R, Tseng M: Association of transcription factor YY1 with the high molecular weight Notch complex suppresses the transactivation activity of Notch. J Biol Chem 2003;278:41963-41969.

21 Franken N, Rodermond H, Stap J, Haveman J, van Bree C: Clonogenic assay of cells *in vitro*. Nat Protoc 2006;1:2315-2319.
22 Ikushima H, Todo T, Ino Y, Takahashi M, Miyazawa K, Miyazono K: Autocrine TGF-beta signaling maintains tumorigenicity of glioma-initiating cells through Sry-related HMG-box factors. Cell Stem Cell 2009;5:504-514.
23 Lu J, He M, Wang L, Chen Y, Liu X, Dong Q, Chen Y, Peng Y, Yao K, Kung H, Li X: MiR-26a inhibits cell growth and tumorigenesis of nasopharyngeal carcinoma through repression of EZH2. Cancer Res 2011;71:225-233.
24 Ordóñez-Morán P, Dafflon C, Imajo M, Nishida E, Huelsken J: HOXA5 Counteracts Stem Cell Traits by Inhibiting Wnt Signaling in Colorectal Cancer. Cancer Cell 2015;28:815-829.
25 Huang J, Xiao D, Li G, Ma J, Chen P, Yuan W, Hou F, Ge J, Zhong M, Tang Y, Xia X, Chen Z: EphA2 promotes epithelial-mesenchymal transition through the Wnt/β-catenin pathway in gastric cancer cells. Oncogene 2014;33:2737-2747.
26 Vermeulen L, De Sousa E Melo F, van der Heijden M, Cameron K, de Jong J, Borovski T, Tuynman J, Todaro M, Merz C, Rodermond H, Sprick M, Kemper K, Richel D, Stassi G, Medema J: Wnt activity defines colon cancer stem cells and is regulated by the microenvironment. Nat Cell Biol 2010;12:468-476.
27 Bartel DP: MicroRNAs: genomics, biogenesis, mechanism, and function. Cell 2004;116:281-297.
28 Garofalo M, Quintavalle C, Di Leva G, Zanca C, Romano G, Taccioli C, Liu C, Croce C, Condorelli G: MicroRNA signatures of TRAIL resistance in human non-small cell lung cancer. Oncogene 2008;27:3845-3855.
29 Calin G, Sevignani C, Dumitru C, Hyslop T, Noch E, Yendamuri S, Shimizu M, Rattan S, Bullrich F, Negrini M, Croce C: Human microRNA genes are frequently located at fragile sites and genomic regions involved in cancers. Proc Natl Acad Sci USA 2004;101:2999-3004.
30 Clarke MF, Dick JE, Dirks PB, Eaves CJ, Jamieson CH, Jones DL, Visvader J, Weissman IL, Wahl GM: Cancer stem cells--perspectives on current status and future directions: AACR Workshop on cancer stem cells. Cancer Res 2006;66:9339-9344.
31 Ward R, Dirks P: Cancer stem cells: at the headwaters of tumor development. Annu Rev Pathol 2007;2:175-189.